

Stockholm
USITP 96-4
April 1996

MAKING ANTI-DE SITTER BLACK HOLES

Stefan Åminneborg¹

Ingemar Bengtsson²

Sören Holst³

Peter Peldán⁴

*Fysikum
Stockholm University
Box 6730, S-113 85 Stockholm, Sweden*

Abstract

It is known from the work of Bañados et al. that a space-time with event horizons (much like the Schwarzschild black hole) can be obtained from 2+1 dimensional anti-de Sitter space through a suitable identification of points. We point out that this can be done in 3+1 dimensions as well. In this way we obtain black holes with event horizons that are tori or Riemann surfaces of genus higher than one. They can have either one or two asymptotic regions. Locally, the space-time is isometric to anti-de Sitter space.

¹Email address: stefan@vanosf.physto.se

²Email address: ingemar@vana.physto.se

³Email address: holst@vanosf.physto.se

⁴Email address: peldan@vanosf.physto.se

It came as a surprise when Bañados et al. produced a “black hole” solution of Einstein’s equations, with a negative cosmological constant, in 2+1 dimensions [1]. This was unexpected because all such solutions are locally isometric to anti-de Sitter space, which has constant curvature. Indeed the solution can be obtained by a suitable identification of points in anti-de Sitter space. The original papers spawned a rather large literature (reviewed recently by Carlip and by Mann [2]), but it appears to have gone unnoticed that the construction can be generalized to higher dimensions, in particular to four dimensions. Our purpose here is to remedy this deficiency. It will become evident as we proceed that the essential ingredient which makes the construction possible is the peculiar asymptotic structure of anti-de Sitter space, which has a timelike boundary at spatial infinity. The dimension of space-time is not essential.

We wish to acknowledge the work of Brill and Steif [3], who stressed that it is helpful to look at the BHTZ construction from an initial data point of view.

Before we begin our construction we give a thumbnail sketch of anti-de Sitter space. It is defined as the surface

$$X^2 + Y^2 + Z^2 - U^2 - V^2 = -1 \quad (1)$$

embedded in a five dimensional flat space with the metric

$$ds^2 = dX^2 + dY^2 + dZ^2 - dU^2 - dV^2 . \quad (2)$$

This is a solution of Einstein’s equations with the cosmological constant $\Lambda = -3$. Its intrinsic curvature is constant and negative. We find it helpful to think sometimes in terms of the coordinates in the embedding space, and sometimes in terms of the intrinsic coordinates (t, ρ, θ, ϕ) , where [4]

$$\begin{aligned} X &= \frac{2\rho}{1-\rho^2} \sin \theta \cos \phi & 0 \leq \rho < 1 \\ Y &= \frac{2\rho}{1-\rho^2} \sin \theta \sin \phi & 0 \leq \phi < 2\pi \\ Z &= \frac{2\rho}{1-\rho^2} \cos \theta & 0 \leq \theta \leq \pi \\ U &= \frac{1+\rho^2}{1-\rho^2} \cos t & 0 \leq t < 2\pi . \\ V &= \frac{1+\rho^2}{1-\rho^2} \sin t \end{aligned} \quad (3)$$

Most of our reasoning will employ the embedding coordinates, but we will use the intrinsic coordinates for drawing the pictures. The intrinsic coordinates cover all of space-time, and in terms of them the intrinsic metric is

$$ds^2 = - \left(\frac{1 + \rho^2}{1 - \rho^2} \right)^2 dt^2 + dl^2 , \quad (4)$$

where

$$dl^2 = \frac{4}{(1 - \rho^2)^2} (d\rho^2 + \rho^2 d\theta^2 + \rho^2 \sin^2 \theta d\phi^2) . \quad (5)$$

The metric dl^2 is the metric on hyperbolic three-space represented as the interior of a unit ball. We refer to this ball as the Poincaré ball, since it is the generalization to three dimensions of the Poincaré disk as a model for Lobachevskian geometry (which was reviewed for physicists by Balasz and Voros [5]). Hyperbolic three-space can be defined as one sheet of the hyperboloid

$$X^2 + Y^2 + Z^2 - U^2 = -1 \quad (6)$$

embedded in flat Minkowski space. In our coordinate system anti-de Sitter space has been foliated with Poincaré balls having zero extrinsic curvature.

Some elementary facts about hyperbolic three-space will be used below. Its geodesics are segments of circles orthogonal to the boundary of the Poincaré ball. Its isometries are elements of $SO(3, 1)$ which we call rotations and boosts, using a terminology familiar from the study of the Lorentz group. A boost can be characterized as an isometry that has two fixed points, both situated on the boundary of the ball. Some elementary facts about anti-de Sitter space will also be needed, in particular the fact that a light ray that passes the spatial origin at time $t = 0$ will strike spatial infinity at $t = \pi/2$. Conversely, the future domain of dependence of the hypersurface $t = 0$ ends at $t = \pi/2$, because of information leaking in from infinity.

We now turn to a description of the black hole found by Bañados et al. [1]. They work in 2+1 dimensional anti-de Sitter space, which can of course be obtained as the intersection of the hypersurface $Z = 0$ with the four dimensional space-time given above. To obtain their black hole (more precisely what they call their spinless black hole, and what we will call the BHTZ space-time) one will have to identify points that can be connected with each other by an isometry generated by the Killing vector

$$J_{XU} = X\partial_U + U\partial_X . \quad (7)$$

The Killing vector field is time-like in a part of space-time. The “identification surfaces” are chosen in such a way that there are no closed time-like curves in the solution, which means that they should lie entirely within

the region where the Killing vector field is space-like. This we will call the “allowed region” — the covering manifold of the BHTZ space-time. It is given by

$$U^2 > X^2 . \quad (8)$$

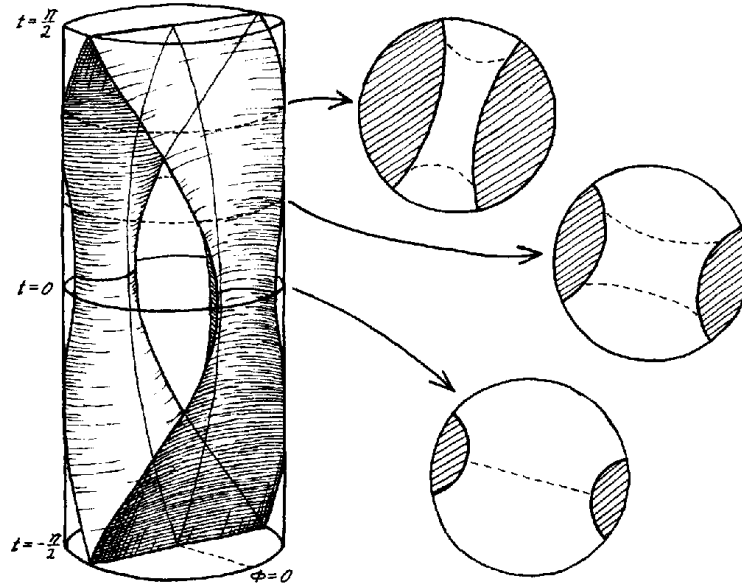


Fig. 1. The 2+1 dimensional (spinless) BHTZ solution in coordinates (t, ρ, ϕ) defined in (3) (where $\theta = \pi/2$ since $Z = 0$). All points inside the cylinder belong to anti-de Sitter space, its surface ($\rho = 1$) representing spatial infinity. The BHTZ spacetime lies between the two surfaces inside the cylinder which are identified under an isometry generated by (7). Since this isometry has fixpoints at $\phi = \pi/2, t = \pm\pi/2$ the surfaces merge and we have singularities there. The future singularity is hidden by an event horizon which “splits up” at $t = 0$. This horizon is indicated by the dashed lines in the constant time slices to the right.

In figure 1 we have depicted a pair of suitable surfaces. They can be obtained by moving the “vertical” hypersurface $X = 0$ backwards or forwards along the Killing vector field, and are given by the equation

$$\frac{X}{U} = \tanh u \quad (9)$$

for suitable values of the constant u . Identifying corresponding points on these surfaces gives us the BHTZ space-time. The region bounded by the

identification surfaces is a regular solution of Einstein’s equations which is locally isometric to anti-de Sitter space. However, when the surfaces merge (at $t = \pm\pi/2$) the quotient space becomes singular and the BHTZ space-time ends there. The singularities are of the “Misner type” [6] — they are clearly not curvature singularities. There are two asymptotic regions in the directions of positive and negative Y , and the space-time topology is $\mathbf{R}^2 \otimes \mathbf{S}^1$.

To see why this is a black hole, consider a light ray that starts out from the origin at time $t = 0$. As we observed above, this light ray will strike spatial infinity at $t = \pi/2$. If we look into the BHTZ space-time from the asymptotic region lying in the positive Y direction nothing that passes the $t = 0$ hypersurface with a negative Y value can be seen — we have an event horizon and therefore a black hole. The location of the event horizon at three different times are shown by the dashed lines on the spatial slices depicted in figure 1. Evidently, the Penrose diagram is that drawn in figure 2. Note that this is the same Penrose diagram as that of the Schwarzschild-anti-de Sitter solution. The Penrose diagram of anti-de Sitter space is also shown, for comparison.

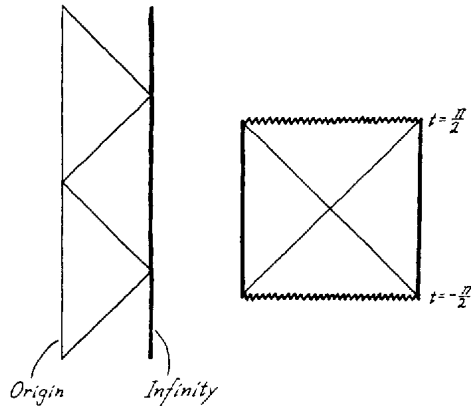


Fig. 2. The Penrose diagrams of anti-de Sitter space and the BHTZ solution respectively. Note that the latter has two disconnected infinities.

We are now ready to study the situation in four dimensions. In our first construction we simply rotate the BHTZ space-time around the X -axis. The identification surfaces are still given by eq. (9). Again the two surfaces merge at $t = \pm\pi/2$, so our space-time begins and ends in singularities at these times. To visualize the resulting space-time, figure 3 may be helpful. It shows the location of the identification surfaces in the Poincaré balls at three different values of t (the first picture is taken at $t = 0$). The main new

feature compared to 2+1 dimensions is that spatial infinity is connected — there is only one asymptotic region in 3+1 dimensions.

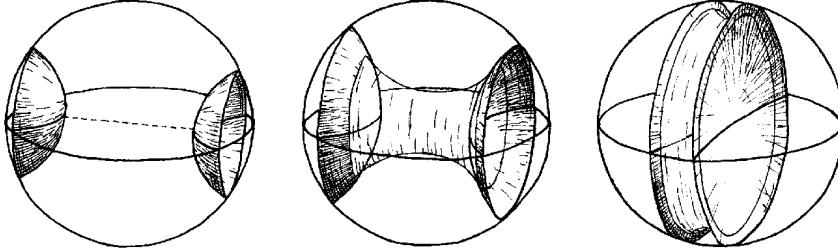


Fig. 3. The 3+1 dimensional generalization of the BHTZ solution in the coordinates (ρ, θ, ϕ) defined in (3) at three different times. In these coordinates, at each time, space is a Poincaré ball and the identification surfaces segments of spheres, meeting the boundary at right angles. As before an event horizon grows up at $t = 0$. In fact, these pictures are obtained simply by rotating the constant time slices in figure 1 around $\phi = 0$.

Now watch the dashed line — actually it is a circle — that connects the identification surfaces at $t = 0$. Photons emitted from this line will reach spatial infinity at $t = \pi/2$, which is the time when space-time ends in a singularity. It is clear that a toroidal event horizon will grow up from this line, as shown in the two subsequent Poincaré balls in figure 3. This is quite similar to the 2+1 dimensional solution, but due to the fact that there is now only one asymptotic region there is also an important difference. The Penrose diagram is given in figure 4. Unlike its 2+1 dimensional counterpart this is not an eternal black hole.

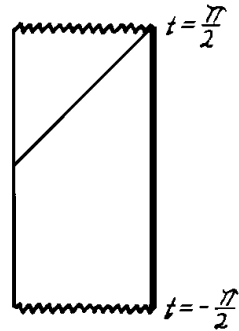


Fig. 4. The Penrose diagram of the 3+1 dimensional BHTZ solution. In contrast to the 2+1 dimensional case, depicted in figure 2, we now have only one infinity.

Our next example is less trivial. We will identify points that can be connected by a discrete subgroup Γ of the $SO(2,1)$ group of isometries generated by the Killing vectors J_{XU}, J_{YU} and J_{XY} . The “identification surfaces” must lie in the region where the three Killing vector fields are

spacelike, that is to say that the allowed region is defined by

$$U^2 > X^2 + Y^2 . \quad (10)$$

It is clear that the hypersurface defined by eq. (9), and hypersurfaces obtained from it by performing rotations generated by the Killing vector J_{XY} , are suitable choices. The solution will then necessarily be singular at $t = \pm\pi/2$, because at those times every identification surface will form a plane containing the Z -axis and going straight through the middle of the Poincaré ball.

It is necessary to exercise some care to ensure that these are the only singularities that arise. Consider first a simpler case, that of a hyperbolic plane \mathbf{H}^2 defined by

$$\hat{X}^2 + \hat{Y}^2 - \hat{U}^2 = -1 . \quad (11)$$

It is well known [5] that one can select a discrete subgroup Γ of boosts in $SO(2,1)$ such that the quotient space $\Sigma = \mathbf{H}^2/\Gamma$ becomes a compact Riemann surface of genus greater than one. The idea is to choose a polygon bounded by geodesics as the fundamental region for the discrete group Γ , whose generators exchange pairs of edges of the polygon. In order to prevent that conical singularities arise in the quotient space the sum of the angles of the polygon has to be equal to 2π . The simplest candidate for a polygon — a square — is ruled out because in the hyperbolic plane the sum of its angles is less than 2π . To do the trick one needs a polygon with $4g$ sides, where $g \geq 2$. The sum of the angles can then always be set equal to 2π by adjusting the size of the polygon, since the angles shrink as the area of the polygon increases. The regular surface that arises when the edges have been identified is then a compact Riemann surface of genus g .

The simplest possible case is that of a regular octagon with opposing edges identified, as illustrated in figure 5. An elementary calculation shows that the Euclidean coordinate distance d between the origin and the symmetrically placed edges has to be

$$d = \sqrt{\sqrt{2} - 1} \quad (12)$$

(in coordinates where the Euclidean coordinate radius of the disk is unity).

So what we intend to do is to define a two-parameter family of Poincaré disks which is such that every point in the allowed region — defined by eq. (10) — lies on a unique disk, and such that each disk is mapped into itself by the $SO(2,1)$ group of isomorphisms generated by J_{XU} , J_{YU} and J_{XY} . Then we select a discrete subgroup Γ of $SO(2,1)$ and use it to compactify all the disks at one stroke. We have to check that all the compactified disks

are smooth manifolds, so that the resulting solution will have the topology $\mathbf{R}^2 \otimes \Sigma$, where Σ is a Riemann surface of genus higher than one.

This is easier than it sounds. First we rewrite the equation that defines anti-de Sitter space as

$$X^2 + Y^2 - U^2 - V^2 = -(1 + Z^2) . \quad (13)$$

We see that Z parametrizes a family of three-dimensional anti-de Sitter spaces that foliate the four-dimensional space. A coordinate system that takes advantage of this situation is

$$Z = \sinh z \quad V = \sin v \cosh z \quad X = R\hat{X} \quad Y = R\hat{Y} \quad U = R\hat{U} \quad (14)$$

where

$$R = R(v, z) = \cos v \cosh z \quad (15)$$

and $(\hat{X}, \hat{Y}, \hat{U})$ obey eq. (11). This coordinate system covers all of the allowed region (where the Killing vector fields we will use for identification are spacelike). In this region the space-time metric then takes the form

$$ds^2 = -\cosh^2 z dv^2 + dz^2 + R^2 d\sigma^2 , \quad (16)$$

where $d\sigma^2$ is the metric on the hyperbolic plane defined by eq. (11). Thus every point in the allowed region lies on a unique disk with a radius of curvature R that depends on z and v . Our $SO(2, 1)$ Killing vectors are

$$J_{XU} = X\partial_U + U\partial_X = \hat{X}\partial_{\hat{U}} + \hat{U}\partial_{\hat{X}} \quad (17)$$

and so on. Therefore they lie in the disks and the intersections of any disk with the level surfaces of the Killing vector fields are geodesics on the disk. Indeed figure 5 applies to all the disks if it applies to one of them, since the radius of curvature does not affect the coordinate distance d . This is all we need to see that our construction works; in particular conditions such as the condition on d given in eq. (12) will be fulfilled on all the disks if it is fulfilled on one.

To visualize the solution consider figure 6, which shows the Poincaré ball defined by $t = 0$. It lies entirely within the allowed region. The identification surfaces are seen as segments of spheres going through the ball. Figure 6 illustrates the simplest case, where the identification surfaces have been chosen so that their intersections with the hyperbolic planes that foliate the ball form regular octagons. The compactified planes will then be compact surfaces of genus two. If we — mentally — add the fourth

dimension to the picture every such compact surface can be thought of as an initial data surface for a solution of Einstein's equations in 2+1 dimensions, giving rise to a locally anti-de Sitter space-time which begins and ends in a singularity.

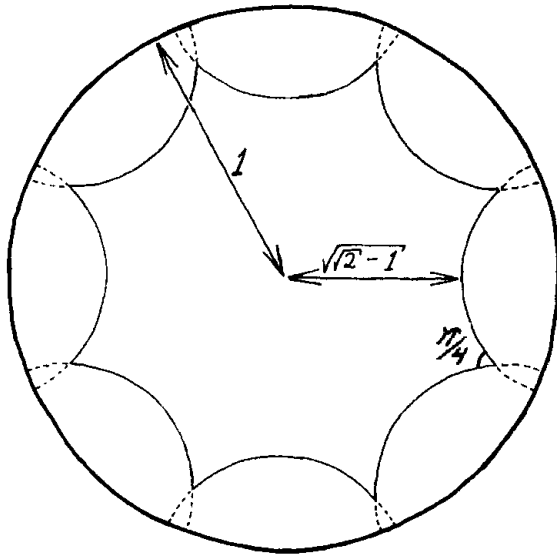


Fig. 5. A regular octagon in the Poincaré disk such that its sum of angles equals 2π . The edges are geodesics. When opposing edges are identified we obtain a surface of genus two, with no singularities.

It remains to locate the event horizons. There are two asymptotic regions in the $\pm Z$ directions. A light ray from the origin has just enough time to reach infinity before the singularity at $t = \pi/2$ terminates the solution, and therefore the origin lies on an event horizon. It is obvious on symmetry grounds that the event horizon at $t = 0$ is precisely the Riemann surface that in figure 6 is depicted as the octagon that lies on the plane that goes through the middle of the ball. This event horizon then splits in two and moves outwards; the Penrose diagram for our solution is the same as the Penrose diagram for the BHTZ solution in figure 2.

We have now completed the constructions that were announced in the abstract of our paper. Our first construction gave non-eternal black holes with toroidal event horizons and one asymptotic region, and the second gave eternal black holes with event horizons of genus higher than one and two asymptotic regions. (Actually a black hole with a toroidal event horizon can be constructed along the lines of the second construction as well,

but it is an extremal black hole with one of the asymptotic regions “replaced” by a singularity.)

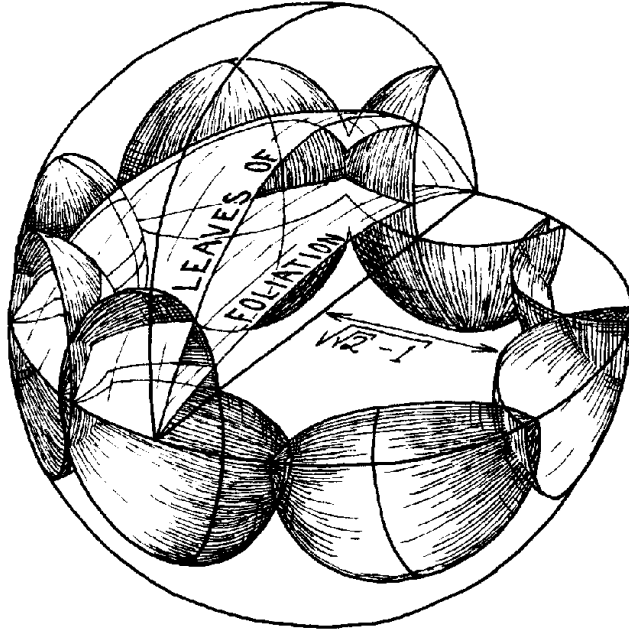


Fig. 6. The Poincaré ball at $t = 0$ (or equivalently $v = 0$). Now the identification surfaces are eight segments of spheres lying inside the ball and meeting its boundary at right angles. As before, opposing surfaces are identified. The “leaves of foliation” indicated in the figure are the surfaces of constant Z at this time, all being the Poincaré disk of figure 5. These leaves are segments of spheres, all containing the equator of the Poincaré ball.

We end with some comments about the possible significance of the black holes that we have made. First of all we see no way to obtain a black hole solution with the topology $\mathbf{R}^2 \otimes \mathbf{S}^2$ through identifications in anti-de Sitter space, and so we are unable to produce a constantly curved black hole with a physically sensible asymptotic behaviour. Therefore (and also because of the sign of the cosmological constant) we conclude that our constructions are of little direct relevance for physics. In particular they are of little relevance to the question of whether — and if so, for how long — event horizons of real black hole can be toroidal (see ref. [7] for recent contributions). On the other hand our black holes appear to be close relatives to the one constructed by Lemos [8], which also requires a space-time with the kind of asymptotic behaviour found in anti-de Sitter space. Whatever

their direct relevance may be, we do believe that our constructions deserve attention as an amusing and perhaps an instructive footnote. Moreover, the occurrence of event horizons in hyperbolic three-spaces is a subject of potential relevance for cosmology.

Acknowledgements:

Ingemar Bengtsson acknowledges Bo Sundborg for an instructive afternoon and the NFR for financial support.

References

- [1] M. Bañados, C. Teitelboim and J. Zanelli, Phys. Rev. Lett. **69** (1992) 1849.
M. Bañados, M. Henneaux, C. Teitelboim and J. Zanelli, Phys. Rev. **D48** (1993) 1506.
- [2] S. Carlip, Class. Quant. Grav. **12** (1995) 2853.
R.B. Mann, Lower Dimensional Black Holes: Inside and Out, gr-qc/9501038, 1995.
- [3] D. Brill, Multi-Black-Hole Geometries in (2+1)-Dimensional Gravity, gr-qc/9511022, 1995.
A. Steif, Time-Symmetric Initial Data for Multi-Body Solutions in Three Dimensions, qr-qc/9511053, 1995.
- [4] S. Holst, Gott Time Machines in the Anti-de Sitter Space, gr-qc/9501010, Gen. Rel. Grav., to appear.
- [5] N.L. Balasz and A. Voros, Phys. Rep. **143** (1986) 109.
- [6] C.W. Misner, in J. Ehlers (ed.): Relativity Theory and Astrophysics, AMS, Providence, R.I. 1967.
- [7] T. Jacobson and S. Venkataramani, Class. Quant. Grav. **12** (1995) 1055.
S.L. Shapiro, S.A. Teukolsky and J. Winicour, Phys. Rev. **D52** (1995) 6982.
- [8] J.P.S. Lemos, Cylindrical Black Hole in General Relativity, gr-qc/9404041, 1994.